

ELECTRONIC SUPPLEMENTARY INFORMATION

Developing strongly luminescent platinum(IV) complexes: facile synthesis of bis-cyclometalated neutral emitters

Fabio Juliá, Delia Bautista, and Pablo González-Herrero*

Contents:

1. Experimental details and characterization data	2
1.1. General Considerations and Materials.....	2
1.2. Analytical Methods.....	2
1.3. Photophysical Characterization	2
1.4. Synthesis and characterization data of new compounds.....	2
1.5. ¹ H-NMR spectra of new compounds (400.9 MHz, CD ₂ Cl ₂).....	7
1.6. X-Ray Structure Determinations	12
1.7. Effect of HCl in the reaction of 1b with PhICl ₂	17
2. Photophysical data	19
2.1. Electronic absorption data of 2a-i	19
2.2. Excitation and emission spectra of 2a-i at 298 K.....	20
2.3. Emission spectra of 2a-i at 77 K	21
2.4. Effect of the concentration on the emission of 2b in solution.....	22
3. Electrochemical characterization of 2b	23
4. Photostability experiments	24
5. References	25

1. Experimental details and characterization data

1.1. General Considerations and Materials

Unless otherwise noted, preparations were carried out under atmospheric conditions. Synthesis grade solvents were obtained from commercial sources. The compounds [Pt₂Me₄(μ-SMe₂)₂],¹ PhICl₂,² 2-(4-methoxyphenyl)pyridine³ (MeOppyH), 5-(dimesitylboranyl)-2-phenylpyridine⁴ (BppyH), 2-(9,9-dimethyl-9*H*-fluoren-2-yl)pyridine⁵ (flpyH), and 2-(1-naphthyl)pyridine⁶ (npyH) were prepared following published procedures. All other reagents were obtained from commercial sources and used without further purification.

1.2. Analytical Methods

NMR spectra were recorded on Bruker Avance 300 or 400 spectrometers at 298 K. Chemical shifts are referred to residual signals of non-deuterated solvent. The number of solvation water molecules was calculated from the integral of the ¹H-NMR water signal, taking into account the water content of the solvent blank. Elemental analyses were carried out with Carlo Erba 1106 and LECO CHNS- 932 microanalyzers.

1.3. Photophysical Characterization

UV-vis absorption spectra were recorded on a Perkin-Elmer Lambda 750S spectrophotometer. Excitation and emission spectra were recorded on a Jobin Yvon Fluorolog 3-22 spectrofluorometer with a 450 W xenon lamp, double-grating monochromators, and a TBX-04 photomultiplier. Solution measurements were carried out in a right angle configuration using 10 mm quartz fluorescence cells or 5 mm quartz NMR tubes at concentrations around 5 × 10⁻⁶ M. For the low-temperature measurements, a liquid nitrogen Dewar with quartz windows was employed. Solutions of the samples were deaerated by bubbling argon for 30 min. Lifetimes were measured using either the Fluorolog's FL-1040 phosphorimeter accessory (τ > 20 μs) or an IBH FluoroHub TCSPC controller and a NanoLED pulse diode excitation source (τ < 20 μs); the estimated uncertainty is ±10% or better. Emission quantum yields were measured using a Hamamatsu C11347 Absolute PL Quantum Yield Spectrometer; the estimated uncertainty is ±5% or better.

1.4. Synthesis and characterization data of new compounds

Synthesis of [PtMe(ppy)(ppyH)] (1b). To a solution of [Pt₂Me₄(μ-SMe₂)₂] (430 mg, 0.75 mmol) in acetone (35 mL) was added ppyH (0.64 mL, 4.48 mmol) and the mixture was refluxed for 4 h. The solvent was removed under reduced pressure and the residue was subjected to three successive dissolution/evaporation cycles using acetone (20 mL) to ensure the removal of Me₂S. Treatment with Et₂O (10 mL) and *n*-pentane (80 mL) led to the

precipitation of a yellow solid, which was filtered off, washed with *n*-pentane (10 mL) and vacuum-dried to give **1b**. Yield: 731 mg, 94%. M.p.: 146 °C. ¹H NMR (400.9 MHz, CD₂Cl₂): δ 9.09 (ddd with satellites, $J_{\text{HH}} = 5.6, 1.7, 0.9$ Hz, $J_{\text{HPt}} \sim 19$ Hz, 1H), 8.05 (m, 2H), 7.98 (td, $J_{\text{HH}} = 7.7, 1.7$ Hz, 1H), 7.80-7.65 (m, 4H), 7.61 (dd with satellites, $J_{\text{HH}} = 7.6, 1.0$ Hz, $J_{\text{HPt}} = 64$ Hz, 1H), 7.50 (m, 1H), 7.43 (ddd, $J_{\text{HH}} = 7.5, 5.6, 1.5$ Hz, 1H), 7.36-7.30 (m, 3 H), 7.08 (m, 1H), 6.99 (m, 1H), 6.92 (ddd, $J_{\text{HH}} = 7.3, 5.5, 1.4$ Hz, 1H), 0.70 (s with satellites, $J_{\text{HPt}} = 85$ Hz, 3H). ¹³C{¹H} NMR (75.5 MHz, CD₂Cl₂): δ 165.0 (C), 161.2 (C), 152.9 ($J_{\text{CPt}} = 14$ Hz, CH), 146.7 ($J_{\text{CPt}} = 15$ Hz, CH), 144.8 (C), 139.7 (C), 137.5 (CH), 137.1 (CH), 133.9 ($J_{\text{CPt}} = 98$ Hz, CH), 129.5 ($J_{\text{CPt}} = 66$ Hz, CH), 129.4 (CH), 127.9 ($J_{\text{CPt}} = 138$ Hz, CH), 127.1 (CH), 124.0 ($J_{\text{CPt}} = 27$ Hz, CH), 123.7 ($J_{\text{CPt}} = 42$ Hz, CH), 122.4 (CH), 122.1 (CH), 118.6 ($J_{\text{CPt}} = 20$ Hz, CH), -13.8 ($J_{\text{CPt}} = 856$ Hz, CH₃). Elemental analysis calcd for C₂₃H₂₀N₂Pt: C, 53.18; H, 3.88; N, 5.39; found: C, 53.27; H, 4.09; N, 5.44.

The rest of complexes **1** were generated and used *in situ* for the preparation of complexes **2** and therefore their isolation is not described.

General one-pot synthesis of complexes 2. To a solution of [Pt₂Me₄(μ-SMe₂)₂] (100 mg, 0.17 mmol) in acetone (20 mL) was added the corresponding N[^]CH ligand (1.04 mmol) and the mixture was refluxed for 4 h. The solvent was removed under reduced pressure and the residue was subjected to three successive dissolution/evaporation cycles using acetone (20 mL) to ensure the removal of Me₂S, and then washed with *n*-pentane (10 mL). CH₂Cl₂ (25 mL), *N,N*-diisopropylethylamine (DIPEA) (80 μL, 0.460 mmol) and PhICl₂ (105 mg, 0.383 mmol) were added in this order and the resultant solution was stirred at room temperature for 1 h. The mixture was then treated with Na₂CO₃, stirred vigorously for 30 minutes and then filtered. The filtrate was concentrated under reduced pressure (10 mL) and *n*-pentane (60 mL) was added to precipitate the corresponding complex **2**, which was collected by filtration, washed with Et₂O (2 × 5 mL) and vacuum-dried.

[Pt(dfppy)₂(Me)Cl] (2a). White solid, 176 mg, 81%. ¹H NMR (300.1 MHz, CD₂Cl₂): δ 9.74 (ddd with satellites, $J_{\text{HH}} = 5.6, 1.7, 0.8$ Hz, $J_{\text{HPt}} \sim 10$ Hz, 1H), 8.40 (apparent d, $J = 8.4$ Hz, 1H), 8.31 (apparent d, $J = 8.5$ Hz, 1H), 8.12 (apparent t, $J = 8.0$ Hz, 1H), 7.82 (apparent t, $J = 8.0$ Hz, 1H), 7.61 (ddd, $J = 5.6, 1.7, 1.2$ Hz, 1H), 7.51 (m, 1H), 7.27 (ddd with satellites, $J_{\text{HH}} = 8.8, 2.4, 0.8$ Hz, $J_{\text{HPt}} = 50$ Hz, 1H), 7.06 (ddd, $J = 5.5, 1.9, 1.1$ Hz, 1H), 6.87 (m, 1H), 6.61 (m, 1H), 6.08 (ddd with satellites, $J_{\text{HH}} = 8.5, 2.5, 0.9$ Hz, $J_{\text{HPt}} = 62$ Hz, 1H), 1.11 (a with satellites, $J_{\text{HPt}} = 67$ Hz, 3H). ¹³C{¹H} NMR (75.45 MHz, CD₂Cl₂): δ 167.2-158.2 (C, several multiplets), 148.2 (CH), 146.3 (CH), 145.9 (m, C), 144.6 (m, C), 140.8 (CH), 139.8 (CH), 124.7-124.1 (m, CH), 123.7 (CH), 115.2 (m, CH), 113.4 (m, CH), 101.2 (m, CH), -1.7 ($J_{\text{CPt}} = 597$ Hz, CH₃). Elemental analysis calcd for C₂₃H₁₅ClF₄N₂Pt: C, 44.14; H, 2.42; N, 4.48; found: C, 44.25; H, 2.63; N, 4.71.

[Pt(ppy)₂(Me)Cl] (2b). White solid, 178 mg, 89%. ¹H NMR (400.9 MHz, CD₂Cl₂): δ 9.72 (d with satellites, $J_{\text{HH}} = 5.6$ Hz, $J_{\text{HPt}} \sim 9$ Hz, 1H), 8.10-8.04 (m, 2H), 7.95 (d, $J = 8.2$ Hz, 1H), 7.83-7.65 (m, 4 H), 7.57 (m, 1H), 7.52 (m, 1H), 7.43 (m, 1H), 7.33 (m, 1H), 7.07-6.99 (m, 2H), 6.85 (m, 1H), 6.49 (dd with satellites, $J_{\text{HH}} = 7.8, 1.0$ Hz, $J_{\text{HPt}} = 53$ Hz, 1H), 1.11 (s with satellites, $J_{\text{HPt}} = 68$ Hz, 3H). ¹³C{¹H} NMR (100.8 MHz, CD₂Cl₂): δ 162.6 (C), 162.1 (C), 148.13 (CH), 146.3 (CH), 143.1 (C), 142.6 (C), 141.7 (C), 141.0 (C), 139.9 (CH), 139.0 (CH), 132.4 ($J_{\text{CPt}} = 57$ Hz, CH), 131.7 ($J_{\text{CPt}} = 55$ Hz, CH), 131.4 ($J_{\text{CPt}} = 64$ Hz, CH), 130.6 ($J_{\text{CPt}} = 36$ Hz, CH), 125.4 ($J_{\text{CPt}} = 33$ Hz, CH), 125.0 ($J_{\text{CPt}} = 37$ Hz, CH), 124.9 (CH), 124.7 ($J_{\text{CPt}} = 7$ Hz, CH), 124.3 ($J_{\text{CPt}} = 10$ Hz, CH), 123.4 ($J_{\text{CPt}} = 7$ Hz, CH), 120.3 ($J_{\text{CPt}} = 7$ Hz, CH), 120.2 ($J_{\text{CPt}} = 7$ Hz, CH), -3.0 ($J_{\text{CPt}} = 624$ Hz, CH₃). Elemental analysis calcd for C₂₃H₁₉ClN₂Pt: C, 49.87; H, 3.46; N, 5.06; found: C, 50.01; H, 3.79; N, 5.33.

[Pt(tpy)₂(Me)Cl] (2c). White solid, 128 mg, 63%. ¹H NMR (300.1 MHz, CD₂Cl₂): δ 9.67 (d with satellites, $J_{\text{HH}} = 5.6$ Hz, $J_{\text{HPt}} \sim 9$ Hz, 1H), 8.06-7.97 (m, 2H), 7.89 (d, $J = 8.0$ Hz, 1H), 7.75-7.66 (m, 2H), 7.62-7.45 (m, 2H), 7.15 (d, $J = 8.0$ Hz, 1H), 6.95 (ddd, $J = 6.9, 5.5, 1.2$ Hz, 1H), 6.87 (m, 1H), 6.33 (s with satellites, $J_{\text{HPt}} = 54$ Hz, 1H), 2.51 (s, 3H), 2.06 (s, 3H), 1.09 (s with satellites, $J_{\text{HPt}} = 68$ Hz, 3H). ¹³C{¹H} NMR (75.45 MHz, CD₂Cl₂): δ 162.6 (C), 162.3 (C), 148.0 (CH), 146.1 (CH), 143.1 (C), 142.2 (C), 141.9 (C), 141.7 (C), 139.9 (C), 139.7 (CH), 138.8 (CH), 138.3 (C), 133.1 ($J_{\text{CPt}} = 58$ Hz, CH), 131.2 ($J_{\text{CPt}} = 38$ Hz, CH), 125.8-125.5 (CH), 125.2 ($J_{\text{CPt}} = 34$ Hz, CH), 124.8 ($J_{\text{CPt}} = 38$ Hz, CH), 123.7 (CH), 122.9 (CH), 120.0 (CH), 119.9 (CH), 22.1 (CH₃), 21.7 (CH₃), -3.2 ($J_{\text{CPt}} = 626$ Hz, CH₃). Elemental analysis calcd for C₂₅H₂₃ClN₂Pt: C, 51.59; H, 3.98; N, 4.81; found: C, 51.62; H, 3.90; N, 4.77.

[Pt(MeOppy)₂(Me)Cl] (2d). White solid, 183 mg, 86%. ¹H NMR (400.9 MHz, CD₂Cl₂): δ 9.62 (d with satellites, $J_{\text{HH}} = 5.4$ Hz, $J_{\text{HPt}} \sim 9$ Hz, 1H), 8.00 (m, 1H), 7.91 (d, $J = 8.2$ Hz, 1H), 7.80 (d, $J = 8.2$ Hz, 1H), 7.74 (m, 1H), 7.68 (m, 1H), 7.61 (m, 1H), 7.49-7.43 (m, 2H), 7.26 (d with satellites, $J_{\text{HH}} = 2.5$ Hz, $J_{\text{HPt}} = 46$ Hz, 1H), 6.93-6.84 (m, 2H), 6.60 (m, 1H), 6.04 (d with satellites, $J_{\text{HH}} = 2.6$ Hz, $J_{\text{HPt}} = 60$ Hz, 1H), 3.94 (s, 3H), 3.54 (s, 3H), 1.10 (s with satellites, $J_{\text{HPt}} = 68$ Hz, 3H). ¹³C{¹H} NMR (100.8 MHz, CD₂Cl₂): δ 162.5 (C), 162.1 (C), 162.0 (C), 161.5 (C), 147.8 (CH), 146.0 (CH), 145.4 (C), 143.6 (C), 139.7 (CH), 138.7 (CH), 135.5 (C), 133.8 (C), 126.7 ($J_{\text{CPt}} = 39$ Hz, CH), 126.3 ($J_{\text{CPt}} = 43$ Hz, CH), 123.0 ($J_{\text{CPt}} = 10$ Hz, CH), 122.2 ($J_{\text{CPt}} = 7$ Hz, CH), 119.6 ($J_{\text{CPt}} = 14$ Hz, CH), 119.5 ($J_{\text{CPt}} = 16$ Hz, CH), 117.8 ($J_{\text{CPt}} = 62$ Hz, CH), 115.2 ($J_{\text{CPt}} = 40$ Hz, CH), 110.8 (CH), 109.7 (CH), 55.6 (CH₃), 55.2 (CH₃), -3.0 ($J_{\text{CPt}} = 622$ Hz, CH₃). Elemental analysis calcd for C₂₅H₂₃ClN₂O₂Pt: C, 48.90; H, 3.78; N, 4.56; found: C, 48.75; H, 3.85; N, 4.85.

[Pt(Bppy)₂(Me)Cl] (2e). Off-white solid, 222 mg, 61%. ¹H NMR (400.9 MHz, CD₂Cl₂): δ 9.62 (dd with satellites, $J_{\text{HH}} = 1.7, 0.7$ Hz, $J_{\text{HPt}} \sim 10$ Hz, 1H), 7.90 (d, $J = 7.8$ Hz, 1H), 7.84 (m, 2H), 7.82-7.68 (m, 4H), 7.44 (m, 1H), 7.39 (dd with satellites, $J_{\text{HH}} = 1.7, 0.7$ Hz, $J_{\text{HPt}} \sim 8$ Hz, 1H), 7.32 (m, 1H), 7.10 (m, 1H), 6.89 (s, 4H), 6.87 (m, 1H), 6.71 (br, 4H), 6.50 (dd with

satellites, $J_{\text{HH}} = 7.8, 1.0$ Hz, $J_{\text{HPt}} = 52$ Hz, 1H), 2.32 (s, 6H), 2.20 (br, 6H), 2.01 (s, 12H), 1.80 (br, 12H), 1.13 (s with satellites, $J_{\text{HPt}} = 69$ Hz, 3H). $^{13}\text{C}\{^1\text{H}\}$ NMR (100.8 MHz, CD_2Cl_2): δ 164.2 (C), 163.8 (C), 157.0 (CH), 154.2 (CH), 147.6 (CH), 146.4 (CH), 144.8 (C), 143.6 (C), 142.3 (C), 141.1 (C), 141.0 (C), 140.8 (C), 140.3 (C), 140.0 (C), 139.7 (C), 138.6 (C), 137.7 (C), 132.4 ($J_{\text{CPt}} = 56$ Hz, CH), 132.1 ($J_{\text{CPt}} = 64$ Hz, CH), 130.7 ($J_{\text{CPt}} = 36$ Hz, CH), 128.9 (CH), 128.8 (CH), 126.1 ($J_{\text{CPt}} = 32$ Hz, CH), 125.7 ($J_{\text{CPt}} = 36$ Hz, CH), 124.9 (CH), 119.7 ($J_{\text{CPt}} = 13$ Hz, CH), 24.0 (CH_3), 21.3 (CH_3), 21.3 (CH_3), -3.4 ($J_{\text{CPt}} = 626$ Hz, CH_3). Elemental analysis calcd for $\text{C}_{59}\text{H}_{61}\text{B}_2\text{ClN}_2\text{Pt}$: C, 67.47; H, 5.85; N, 2.67; found: C, 67.22; H, 5.62; N, 2.91.

[Pt(flpy)₂(Me)Cl] (2f). Beige solid, 242 mg, 89%. ^1H NMR (400.9 MHz, CD_2Cl_2): δ 9.75 (ddd with satellites, $J_{\text{HH}} = 5.6, 1.7, 0.7$ Hz, $J_{\text{HPt}} \sim 10$ Hz, 1H), 8.20 (s with satellites, $J_{\text{HPt}} = 42$ Hz, 1H), 8.15 (d, $J = 8.1$ Hz, 1H), 8.09 (m, 1H), 8.05 (d, $J = 8.3$ Hz, 1H), 7.94 (s, 1H), 7.91 (m, 1H), 7.79-7.73 (m, 2H), 7.60-7.54 (m, 3H), 7.40 (m, 2H), 7.34 (d, $J = 7.4$ Hz, 1H), 7.19 (m, 1H), 7.10-7.04 (m, 2H), 7.00 (ddd, $J = 5.5, 1.9, 1.2$ Hz, 1H), 6.86 (s with satellites, $J_{\text{HPt}} = 55$ Hz, 1H), 1.71 (s, 3H), 1.66 (s, 3H), 1.46 (s, 3H), 1.40 (s, 3H), 1.27 (s with satellites, $J_{\text{HPt}} = 68$ Hz, 3H). $^{13}\text{C}\{^1\text{H}\}$ NMR (100.8 MHz, CD_2Cl_2): δ 162.8 (C), 162.3 (C), 155.1 (C), 154.6 (C), 150.6 (C), 150.0 (C), 148.1 (CH), 146.3 (CH), 142.8 (C), 142.4 (C), 142.3 (C), 141.4 (C), 140.8 (C), 139.7 (CH), 139.6 (C), 139.5 (C), 138.8 (CH), 138.4 (C), 128.1 (CH), 128.0 (CH), 127.4 (CH), 127.1 (CH), 123.8 ($J_{\text{CPt}} = 10$ Hz, CH), 123.6 ($J_{\text{CPt}} = 58$ Hz, CH), 123.0 (CH), 122.9 (CH), 122.8 (CH), 121.9 ($J_{\text{CPt}} = 37$ Hz, CH), 121.2 (CH), 120.5 (CH), 120.3 ($J_{\text{CPt}} = 13$ Hz, CH), 120.1 ($J_{\text{CPt}} = 15$ Hz, CH), 119.8 ($J_{\text{CPt}} = 36$ Hz, CH), 119.2 ($J_{\text{CPt}} = 41$ Hz, CH), 46.9 (C), 46.6 (C), 27.9 (CH_3), 27.4 (CH_3), 27.2 (CH_3), -2.9 ($J_{\text{CPt}} = 625$ Hz, CH_3). Elemental analysis calcd for $\text{C}_{41}\text{H}_{35}\text{ClN}_2\text{Pt}\cdot\text{H}_2\text{O}$: C, 61.23; H, 4.64; N, 3.48; found: C, 60.88; H, 4.36; N, 3.69.

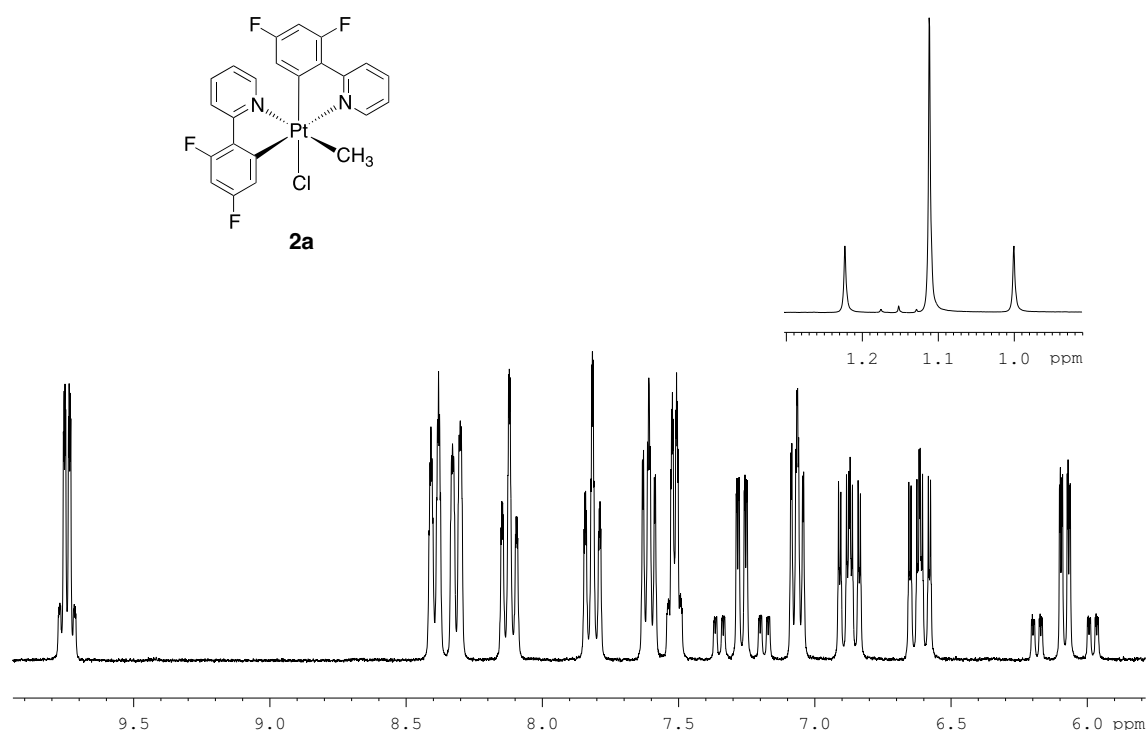
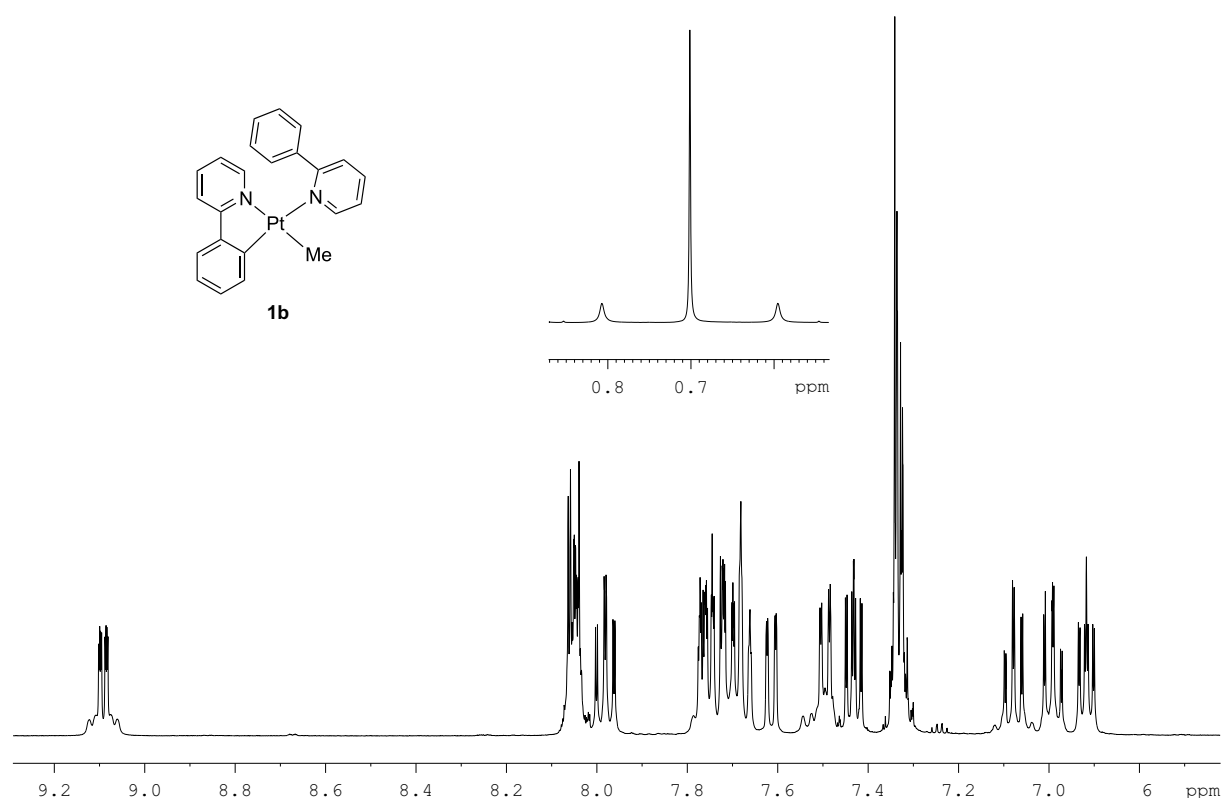
[Pt(thpy)₂(Me)Cl] (2g). White solid, 149 mg, 76%. ^1H NMR (400.9 MHz, CD_2Cl_2): δ 9.49 (ddd with satellites, $J_{\text{HH}} = 5.6, 1.7, 0.9$ Hz, $J_{\text{HPt}} \sim 12$ Hz, 1H), 7.96 (m, 1H), 7.70-7.62 (m, 3H), 7.58-7.52 (m, 2H), 7.40 (m, 1H), 7.34 (d with satellites, $J_{\text{HH}} = 4.9$ Hz, $J_{\text{HPt}} = 16$ Hz, 1H), 7.21 (d with satellites, $J_{\text{HH}} = 4.9$ Hz, $J_{\text{HPt}} = 11$ Hz, 1H), 6.90 (m, 1H), 6.12 (d with satellites, $J_{\text{HH}} = 4.9$ Hz, $J_{\text{HPt}} = 20$ Hz, 1H), 1.30 (s with satellites, $J_{\text{HPt}} = 68$ Hz, 3H). $^{13}\text{C}\{^1\text{H}\}$ NMR (100.8 MHz, CD_2Cl_2): δ 158.9 (C), 157.8 (C), 148.1 (CH), 146.8 (CH), 140.8 (C), 140.3 (CH), 139.4 (CH), 139.0 (CH), 130.1 ($J_{\text{CPt}} = 90$ Hz, CH), 129.7 ($J_{\text{CPt}} = 76$ Hz, CH), 128.9 ($J_{\text{CPt}} = 71$ Hz, CH), 121.9 ($J_{\text{CPt}} = 10$ Hz, CH), 121.4 (CH), 119.1 (CH), -8.1 ($J_{\text{CPt}} = 583$ Hz, CH_3). Elemental analysis calcd for $\text{C}_{19}\text{H}_{15}\text{ClN}_2\text{PtS}_2$: C, 40.32; H, 2.67; N, 4.95; S, 11.33; found: C, 40.50; H, 2.77; N, 4.91; S, 11.55.

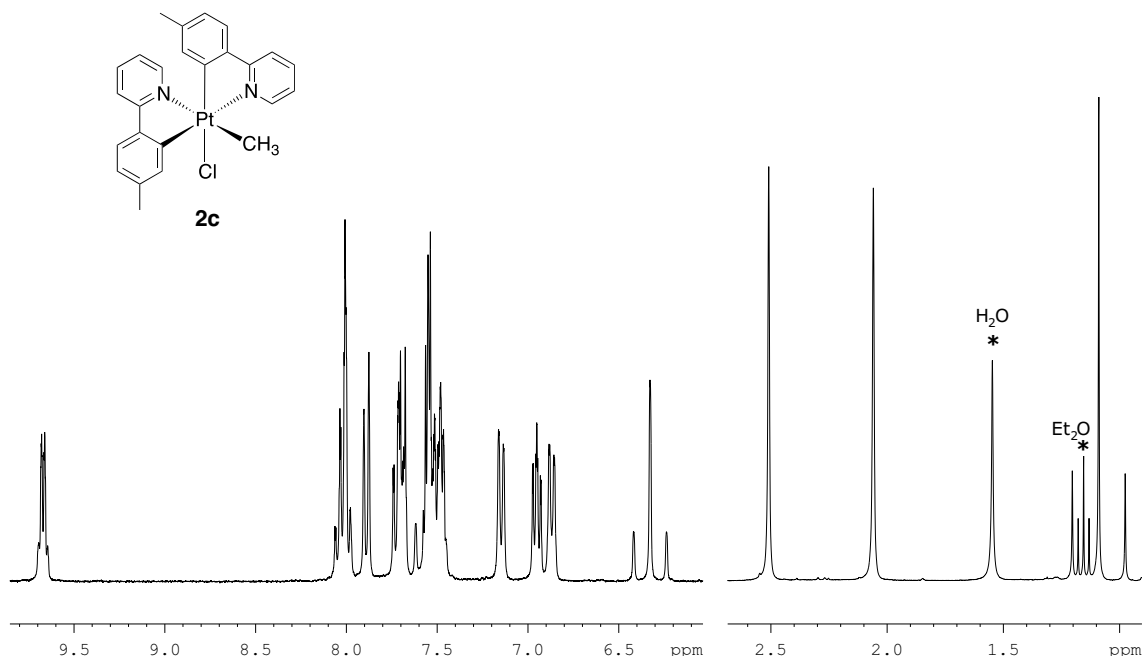
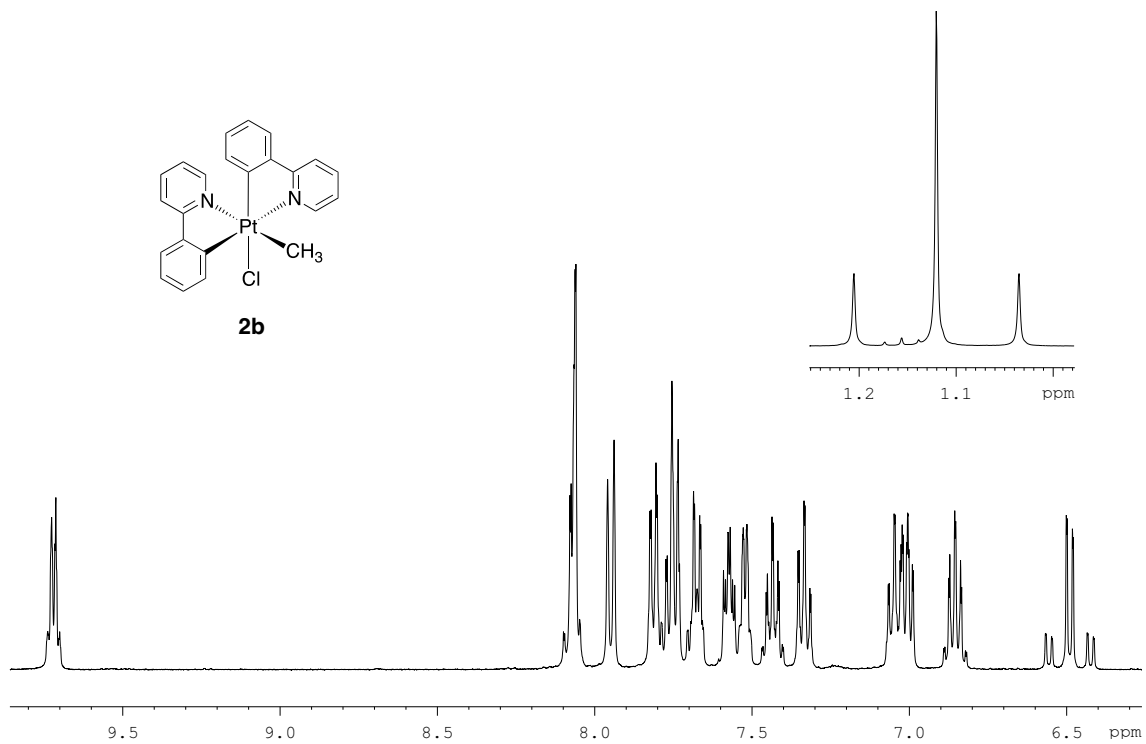
[Pt(piq)₂(Me)Cl] (2h). Yellow solid, 130 mg, 57%. ^1H NMR (400.9 MHz, CD_2Cl_2): δ 9.68 (d with satellites, $J_{\text{HH}} = 6.2$ Hz, $J_{\text{HPt}} = 8.5$ Hz, 1H), 8.98-8.92 (m, 2H), 8.34 (d, $J = 7.8$ Hz, 1H), 8.20 (m, 1H), 8.11 (d, $J = 8.1$ Hz, 1H), 7.97-7.89 (m, 3H), 7.86-7.72 (m, 4H), 7.50 (m, 1H),

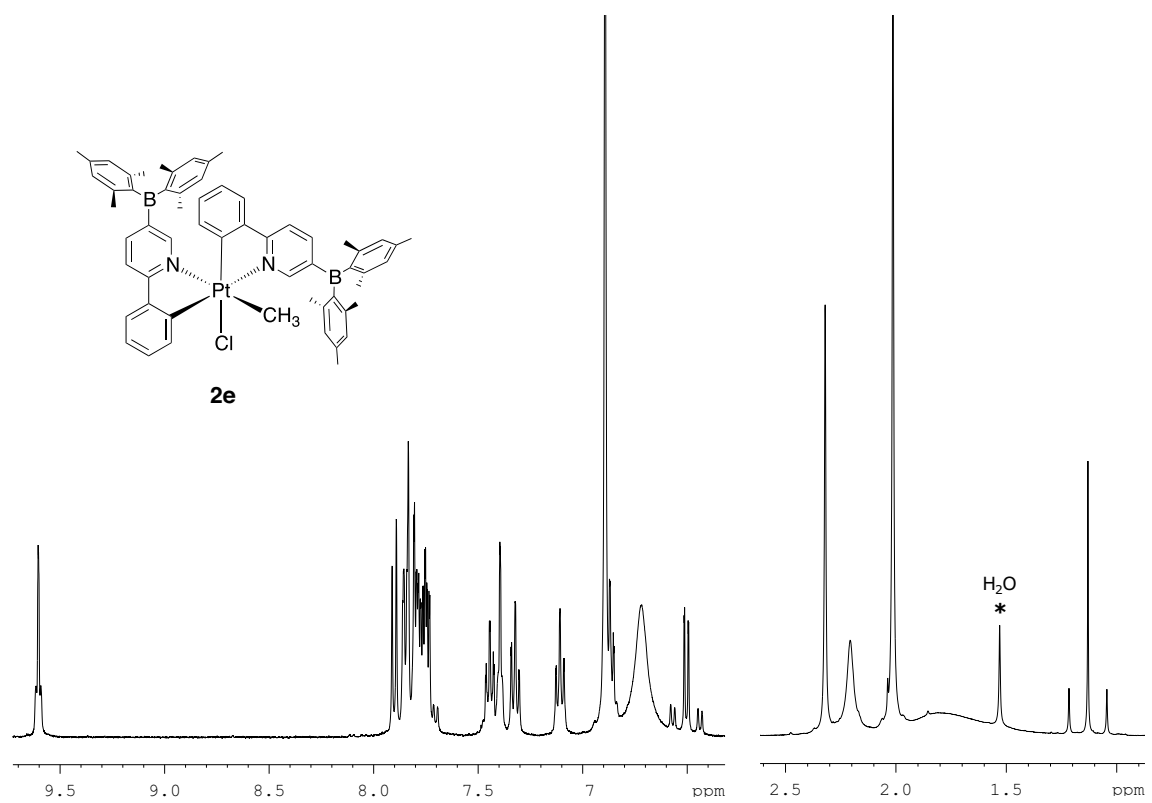
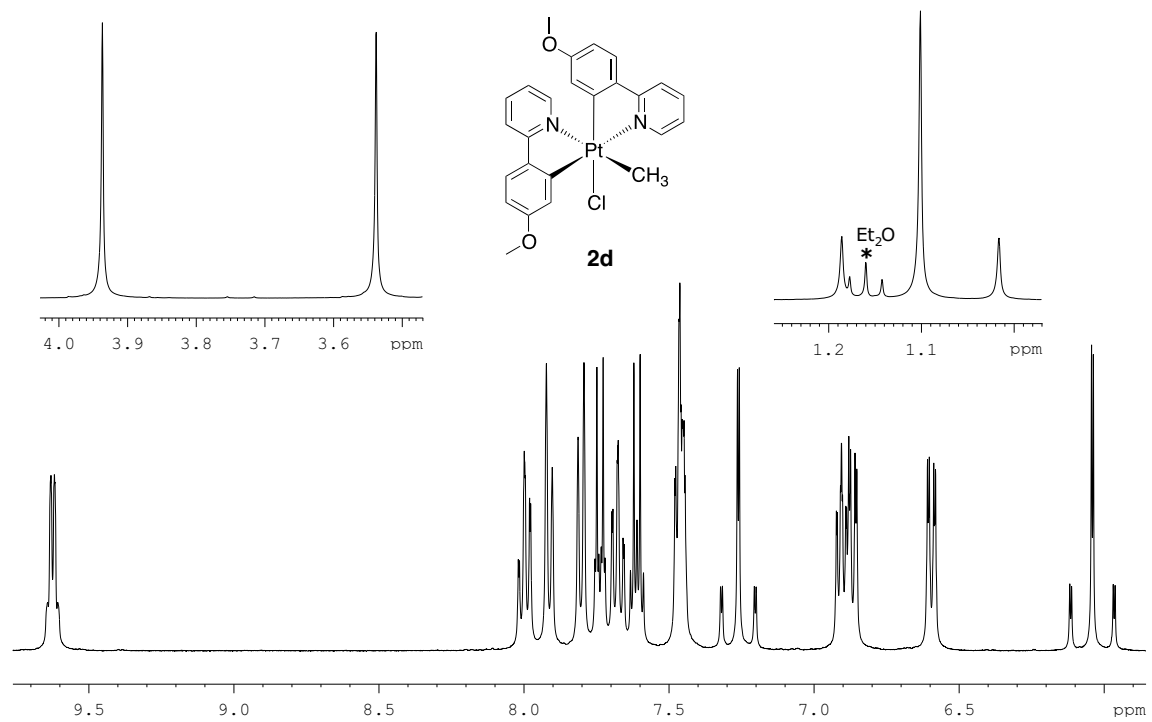
7.45-7.38 (m, 2H), 7.28 (d, $J = 6.2$ Hz, 1H), 7.10 (m, 1H), 6.88 (m, 1H), 6.66 (dd with satellites, $J_{\text{HH}} = 7.8, 1.1$ Hz, $J_{\text{HPt}} = 56$ Hz, 1H), 1.17 (s with satellites, $J_{\text{HPt}} = 68$ Hz, 3H). $^{13}\text{C}\{^1\text{H}\}$ NMR (100.8 MHz, CD_2Cl_2): δ 163.6 (C), 163.5 (C), 145.6 (C), 144.2 (C), 143.9 (C), 142.6 (C), 139.4 (CH), 138.7 (C), 138.1 (CH), 138.0 (C), 132.6 ($J_{\text{CPt}} = 54$ Hz, CH), 132.2 (CH), 131.7 (CH), 131.6 (CH), 131.3 (CH), 131.1 (CH), 131.0 (CH), 130.6 ($J_{\text{CPt}} = 38$ Hz, CH), 129.1 (CH), 128.8 (CH), 128.3 (CH), 127.7 (CH), 127.6 (CH), 127.5 (CH), 126.7 (C), 124.4 (CH), 124.3 (CH), 122.5 (CH), 121.7 (CH), -2.5 ($J_{\text{CPt}} = 626$ Hz, CH_3). Elemental analysis calcd for $\text{C}_{31}\text{H}_{23}\text{ClN}_2\text{Pt}\cdot 0.5 \text{CH}_2\text{Cl}_2$: C, 54.32; H, 3.47; N, 4.02; found: C, 54.17; H, 3.45; N, 4.10.

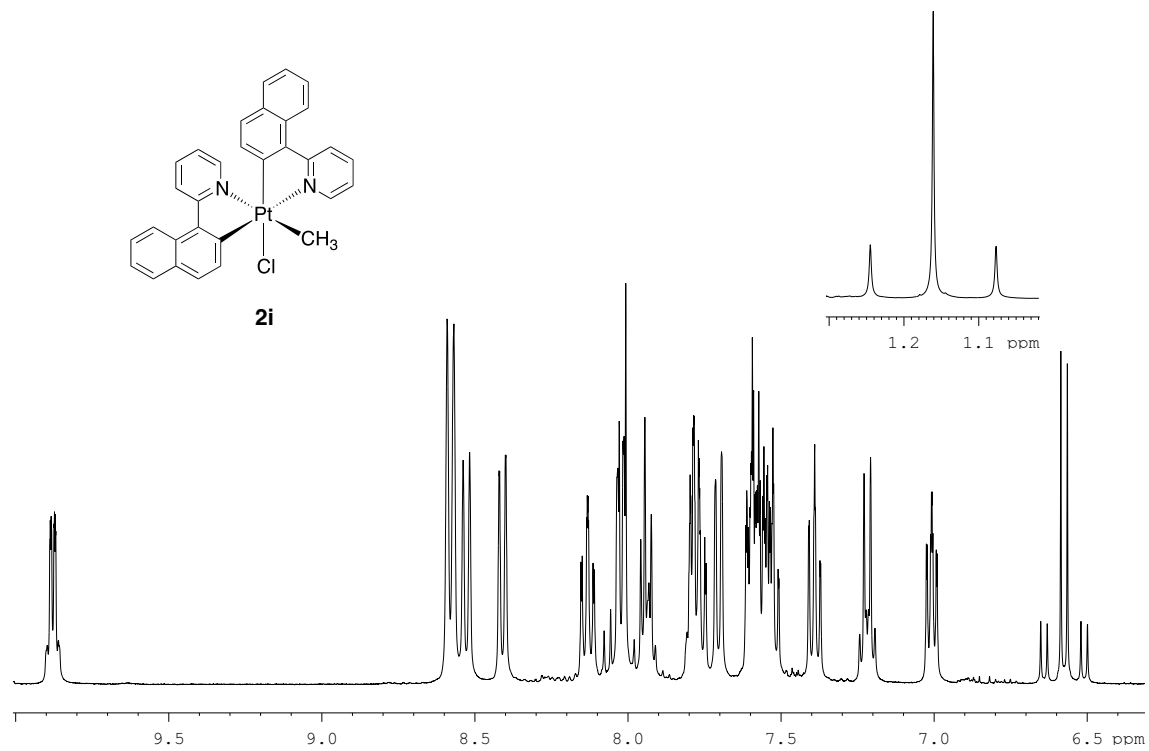
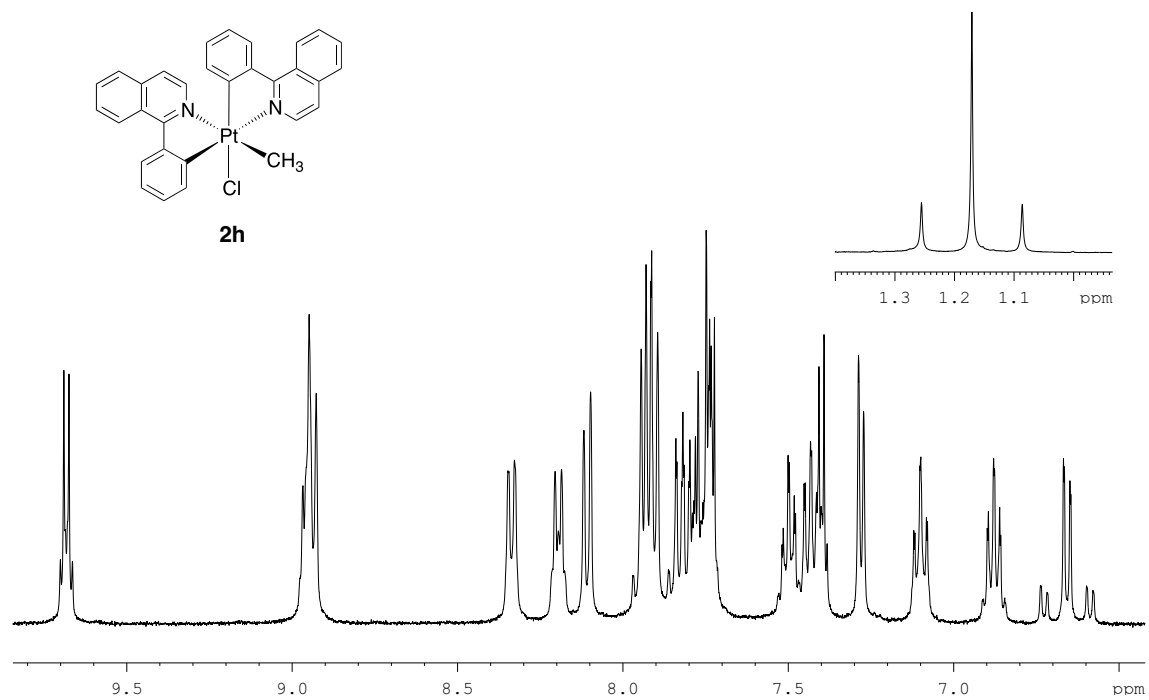
[Pt(np π) $_2$ (Me)Cl] (2i). Beige solid, 142 mg, 62%. ^1H NMR (400.9 MHz, CD_2Cl_2): δ 9.88 (dd with satellites, $J_{\text{HH}} = 5.5, 1.7$ Hz, $J_{\text{HPt}} \sim 10$ Hz, 1H), 8.58 (d, $J = 8.6$ Hz, 1H), 8.53 (d, $J = 8.5$ Hz, 1H), 8.41 (d, $J = 8.3$ Hz, 1H), 8.13 (ddd, $J = 7.5, 1.7, 0.7$ Hz, 1H), 8.08-7.91 (m, 3H), 7.81-7.74 (m, 2H), 7.70 (d, $J = 8.0$ Hz, 1H), 7.62-7.50 (m, 4H), 7.39 (td, $J = 7.4, 0.9$ Hz, 1H), 7.22 (m, 1H), 7.00 (ddd, $J = 5.5, 1.9, 1.1$ Hz, 1H), 6.57 (d with satellites, $J_{\text{HH}} = 8.5$ Hz, $J_{\text{HPt}} = 52$ Hz, 1H), 1.16 (s with satellites, $J_{\text{HPt}} = 68$ Hz, 3H). $^{13}\text{C}\{^1\text{H}\}$ NMR (100.8 MHz, CD_2Cl_2): δ 163.2 (C), 162.7 (C), 149.0 (CH), 147.2 (CH), 146.4 (C), 145.2 (C), 139.6 (CH), 138.7 (CH), 136.9 (C), 135.2 (C), 133.1 (C), 132.5 (C), 131.8 (C), 131.4 ($J_{\text{CPt}} = 53$ Hz, CH), 131.3 (C), 131.0 ($J_{\text{CPt}} = 64$ Hz, CH), 130.4 ($J_{\text{CPt}} = 53$ Hz, CH), 129.8 (CH), 129.6 (CH), 128.6 ($J_{\text{CPt}} = 31$ Hz, CH), 127.5 (CH), 127.3 (CH), 124.9-124.6 (m, CH), 123.5 ($J_{\text{CPt}} = 10$ Hz, CH), 123.1 (CH), 122.9 (CH), 122.7 (CH), -2.1 ($J_{\text{CPt}} = 625$ Hz, CH_3). Elemental analysis calcd for $\text{C}_{31}\text{H}_{23}\text{ClN}_2\text{Pt}$: C, 56.93; H, 3.54; N, 4.28; found: C, 56.88; H, 3.49; N, 4.17.

1.5. $^1\text{H-NMR}$ spectra of new compounds (400.9 MHz, CD_2Cl_2)









1.6. X-Ray Structure Determinations

Crystals of **2a**, **2b**, **2d** and **2f**·CH₂Cl₂ suitable for X-ray diffraction studies were obtained by liquid-liquid diffusion from CH₂Cl₂/Et₂O (**2a**, **2b**) or slow evaporation from a CH₂Cl₂ solution (**2d**, **2f**·CH₂Cl₂). The data were collected on a Bruker D8 QUEST diffractometer with monochromated Mo-*K*α radiation performing φ and ω scans. The structures were solved by direct methods and refined anisotropically on F^2 using the program SHELXL-2013 (**2b**) or SHELXL-2014 (rest of structures) (G. M. Sheldrick, University of Göttingen).⁷ Methyl hydrogens were included as part of rigid idealized methyl groups allowed to rotate but not tip; other hydrogens were included using a riding model. Numerical details are presented in Table S1.

Table S1. Crystallographic Data for **2a**, **2b**, **2d** and **2f**·CH₂Cl₂.

	2a	2b	2d	2f ·CH ₂ Cl ₂
formula	C ₂₃ H ₁₅ ClF ₄ N ₂ Pt	C ₂₃ H ₁₉ ClN ₂ Pt	C ₂₅ H ₂₃ ClN ₂ O ₂ Pt	C ₄₂ H ₃₇ Cl ₃ N ₂ Pt
fw	625.91	553.94	613.99	871.17
<i>T</i> (K)	100(2)	100(2)	100(2)	100(2)
λ (Å)	0.71073	0.71073	0.71073	0.71073
cryst syst	Triclinic	Orthorhombic	Monoclinic	Monoclinic
space group	$P\bar{1}$	<i>Fdd2</i>	$P2_1/n$	$P2_1/c$
<i>a</i> (Å)	8.8700(5)	26.587(3)	10.0073(6)	13.9571(6)
<i>b</i> (Å)	10.7659(6)	40.680(4)	21.4773(12)	14.1969(6)
<i>c</i> (Å)	12.1232(6)	6.9773(7)	11.0633(6)	18.5023(8)
α (deg)	99.7042	90	90	90
β (deg)	109.5047(15)	90	109.9388(19)	102.7354(15)
γ (deg)	104.8861(16)	90	90	90
<i>V</i> (Å ³)	1012.69(10)	7546.2(13)	2235.3(2)	3576.0(3)
<i>Z</i>	2	16	4	4
ρ_{calcd} (Mg m ⁻³)	2.053	1.950	1.824	1.618
μ (mm ⁻¹)	7.109	7.589	6.421	4.181
R1 ^a	0.0162	0.0233	0.0343	0.0175
wR2 ^b	0.0388	0.0370	0.0527	0.0389

^a $R1 = \sum ||F_o| - |F_c|| / \sum |F_o|$ for reflections with $I > 2\sigma(I)$. ^b $wR2 = [\sum [w(F_o^2 - F_c^2)^2] / \sum [w(F_o^2)^2]]^{0.5}$ for all reflections; $w^{-1} = \sigma^2(F^2) + (aP)^2 + bP$, where $P = (2F_c^2 + F_o^2)/3$ and *a* and *b* are constants set by the program.

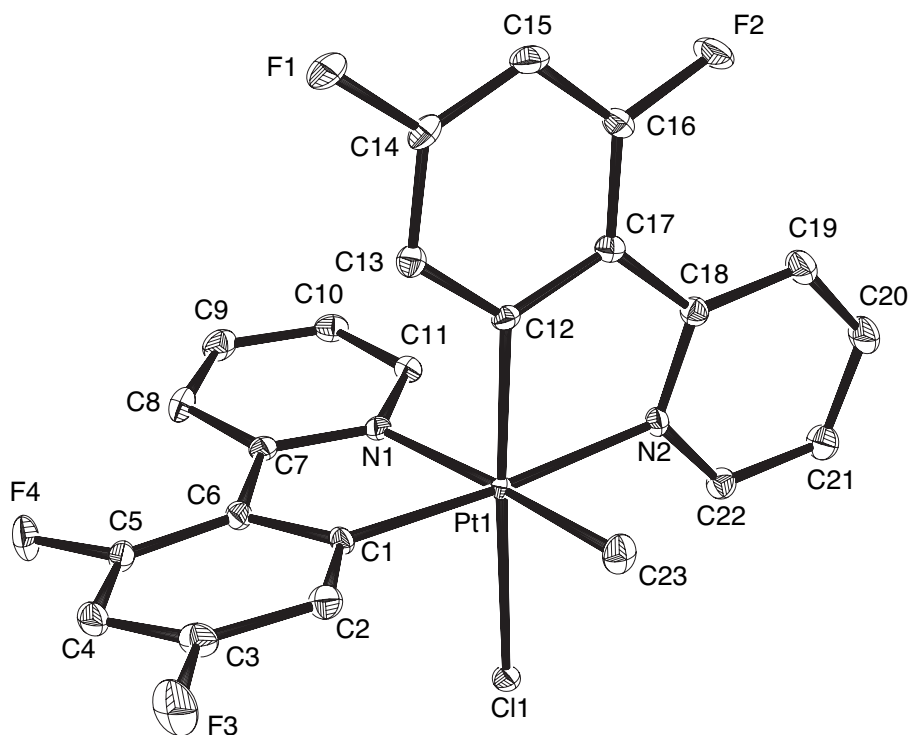


Figure S1. Thermal ellipsoid plot (50% probability) of complex **2a**. Hydrogen atoms are omitted for clarity.

Table S2. Selected bond distances (Å) and angles (deg) in the crystal structure of **2a**.

Pt(1)-C(12)	1.9956(18)	Pt(1)-N(2)	2.1207(15)
Pt(1)-C(1)	2.0113(18)	Pt(1)-N(1)	2.1280(16)
Pt(1)-C(23)	2.0634(19)	Pt(1)-Cl(1)	2.4234(4)
C(12)-Pt(1)-C(1)	95.29(7)	C(23)-Pt(1)-N(1)	174.82(7)
C(12)-Pt(1)-C(23)	89.68(8)	N(2)-Pt(1)-N(1)	98.44(6)
C(1)-Pt(1)-C(23)	94.69(8)	C(12)-Pt(1)-Cl(1)	175.72(5)
C(12)-Pt(1)-N(2)	80.37(7)	C(1)-Pt(1)-Cl(1)	88.79(5)
C(1)-Pt(1)-N(2)	175.51(6)	C(23)-Pt(1)-Cl(1)	91.27(6)
C(23)-Pt(1)-N(2)	86.50(7)	N(2)-Pt(1)-Cl(1)	95.52(4)
C(12)-Pt(1)-N(1)	89.62(7)	N(1)-Pt(1)-Cl(1)	89.80(4)
C(1)-Pt(1)-N(1)	80.27(7)		

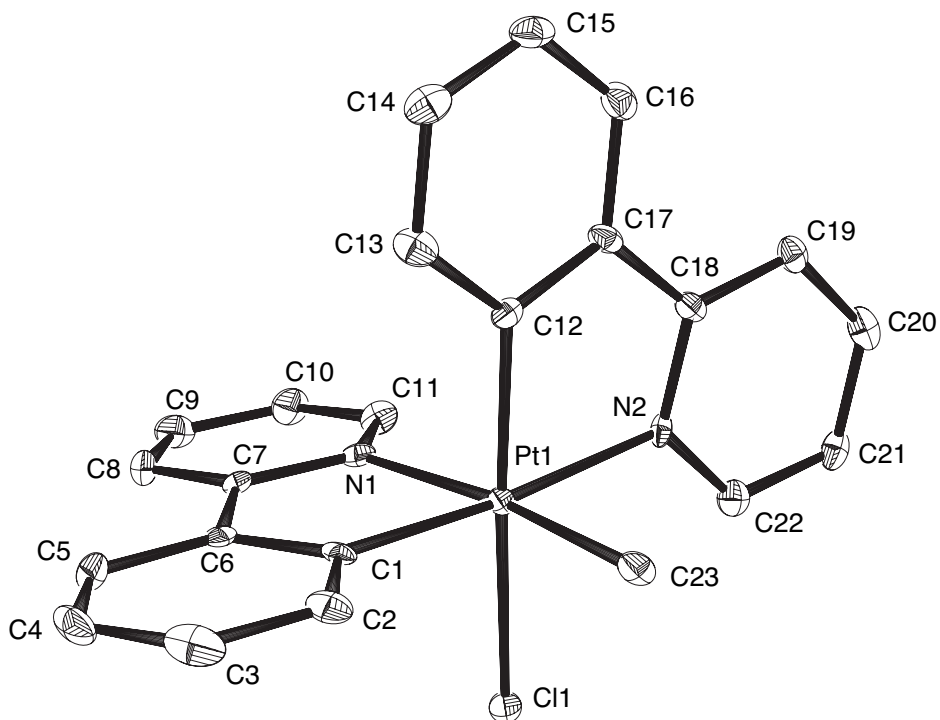


Figure S2. Thermal ellipsoid plot (50% probability) of complex **2b**. Hydrogen atoms are omitted for clarity.

Table S3. Selected bond distances (Å) and angles (deg) in the crystal structure of **2b**.

Pt(1)-C(1)	2.004(6)	Pt(1)-N(1)	2.132(4)
Pt(1)-C(12)	2.009(5)	Pt(1)-N(2)	2.148(4)
Pt(1)-C(23)	2.046(5)	Pt(1)-Cl(1)	2.4372(14)
C(1)-Pt(1)-C(12)	94.0(2)	C(23)-Pt(1)-N(2)	87.52(19)
C(1)-Pt(1)-C(23)	93.0(2)	N(1)-Pt(1)-N(2)	99.04(17)
C(12)-Pt(1)-C(23)	91.9(2)	C(1)-Pt(1)-Cl(1)	91.62(15)
C(1)-Pt(1)-N(1)	80.8(2)	C(12)-Pt(1)-Cl(1)	173.57(16)
C(12)-Pt(1)-N(1)	92.02(18)	C(23)-Pt(1)-Cl(1)	90.93(16)
C(23)-Pt(1)-N(1)	172.9(2)	N(1)-Pt(1)-Cl(1)	85.81(12)
C(1)-Pt(1)-N(2)	174.13(19)	N(2)-Pt(1)-Cl(1)	94.23(12)
C(12)-Pt(1)-N(2)	80.1(2)		

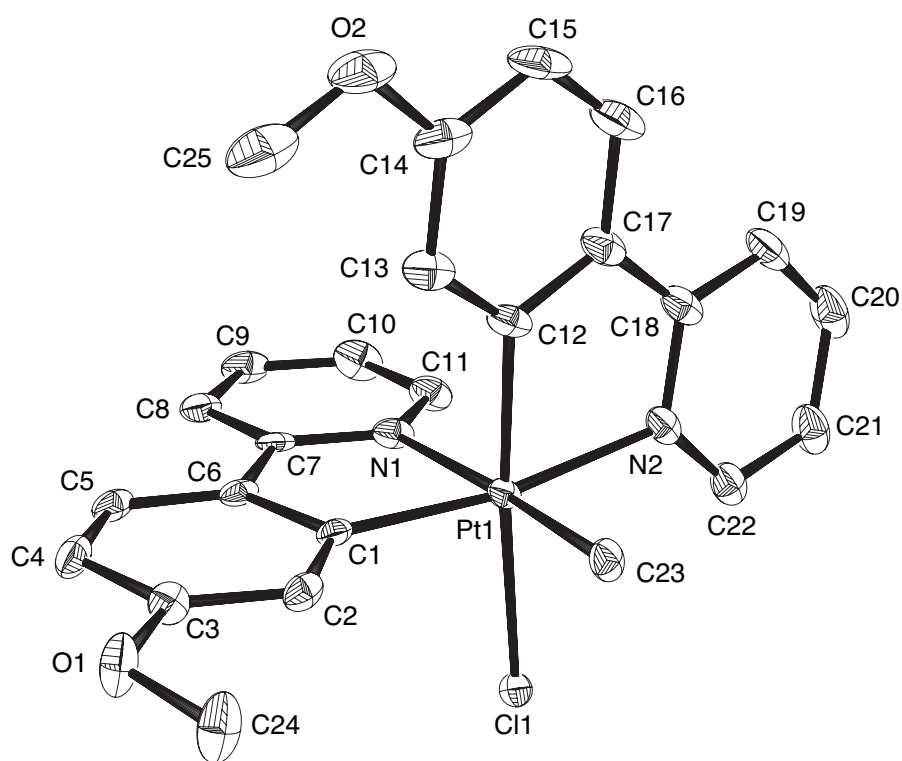


Figure S3. Thermal ellipsoid plot (50% probability) of complex **2d**. Hydrogen atoms are omitted for clarity.

Table S4. Selected bond distances (Å) and angles (deg) in the crystal structure of **2d**.

Pt(1)-C(12)	2.004(4)	Pt(1)-N(2)	2.143(3)
Pt(1)-C(1)	2.005(3)	Pt(1)-N(1)	2.156(3)
Pt(1)-C(23)	2.065(3)	Pt(1)-Cl(1)	2.4369(8)
C(12)-Pt(1)-C(1)	92.84(14)	C(23)-Pt(1)-N(1)	174.61(13)
C(12)-Pt(1)-C(23)	87.56(14)	N(2)-Pt(1)-N(1)	93.13(11)
C(1)-Pt(1)-C(23)	94.27(13)	C(12)-Pt(1)-Cl(1)	175.24(11)
C(12)-Pt(1)-N(2)	80.37(14)	C(1)-Pt(1)-Cl(1)	91.81(9)
C(1)-Pt(1)-N(2)	170.49(12)	C(23)-Pt(1)-Cl(1)	91.09(11)
C(23)-Pt(1)-N(2)	92.09(12)	N(2)-Pt(1)-Cl(1)	95.13(9)
C(12)-Pt(1)-N(1)	91.98(12)	N(1)-Pt(1)-Cl(1)	89.79(8)
C(1)-Pt(1)-N(1)	80.38(12)		

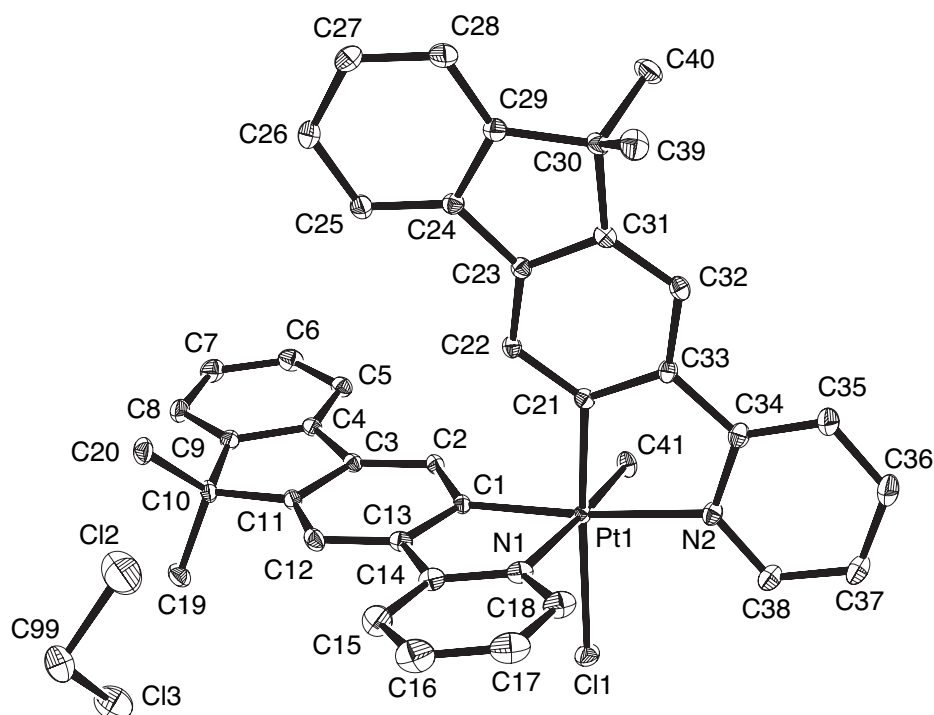


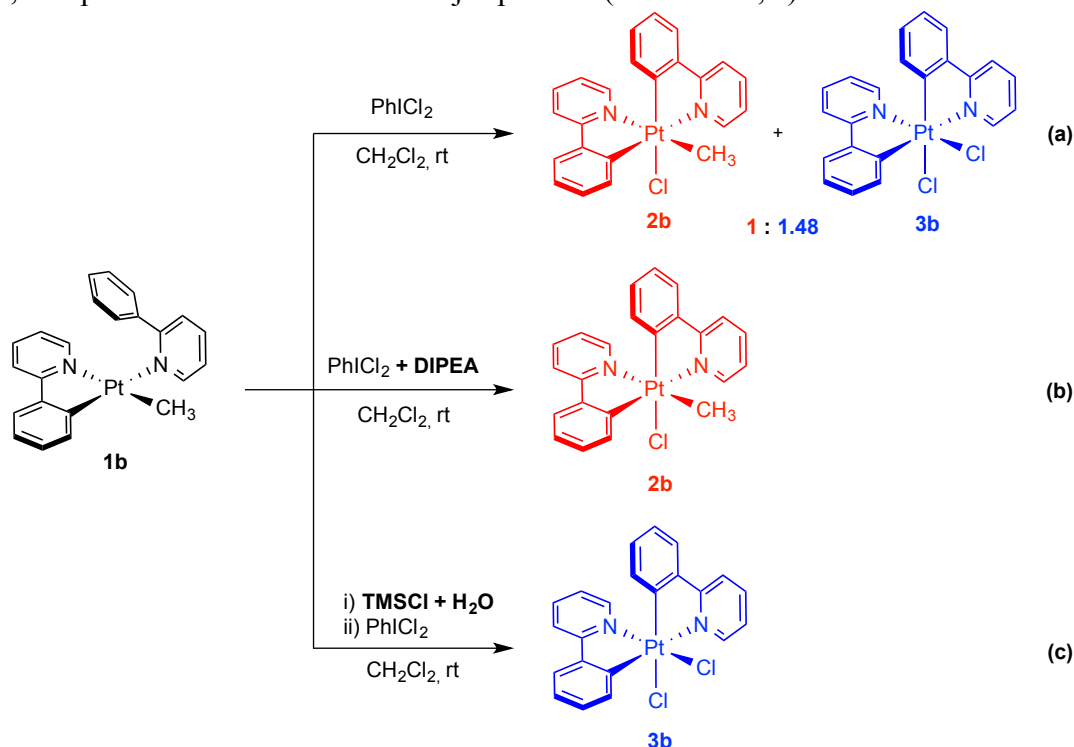
Figure S4. Thermal ellipsoid plot (50% probability) of complex **2f**·CH₂Cl₂. Hydrogen atoms are omitted for clarity.

Table S5. Selected bond distances (Å) and angles (deg) in the crystal structure of **2f**·CH₂Cl₂.

Pt(1)-C(21)	2.0013(15)	Pt(1)-N(2)	2.1308(13)
Pt(1)-C(1)	2.0074(14)	Pt(1)-N(1)	2.1397(13)
Pt(1)-C(41)	2.0556(15)	Pt(1)-Cl(1)	2.4455(4)
C(21)-Pt(1)-C(1)	94.10(6)	C(41)-Pt(1)-N(1)	174.24(6)
C(21)-Pt(1)-C(41)	91.10(6)	N(2)-Pt(1)-N(1)	98.99(5)
C(1)-Pt(1)-C(41)	93.92(6)	C(21)-Pt(1)-Cl(1)	175.15(4)
C(21)-Pt(1)-N(2)	80.07(6)	C(1)-Pt(1)-Cl(1)	89.75(4)
C(1)-Pt(1)-N(2)	174.15(5)	C(41)-Pt(1)-Cl(1)	91.57(5)
C(41)-Pt(1)-N(2)	86.68(6)	N(2)-Pt(1)-Cl(1)	96.05(4)
C(21)-Pt(1)-N(1)	90.86(5)	N(1)-Pt(1)-Cl(1)	86.87(4)
C(1)-Pt(1)-N(1)	80.53(6)		

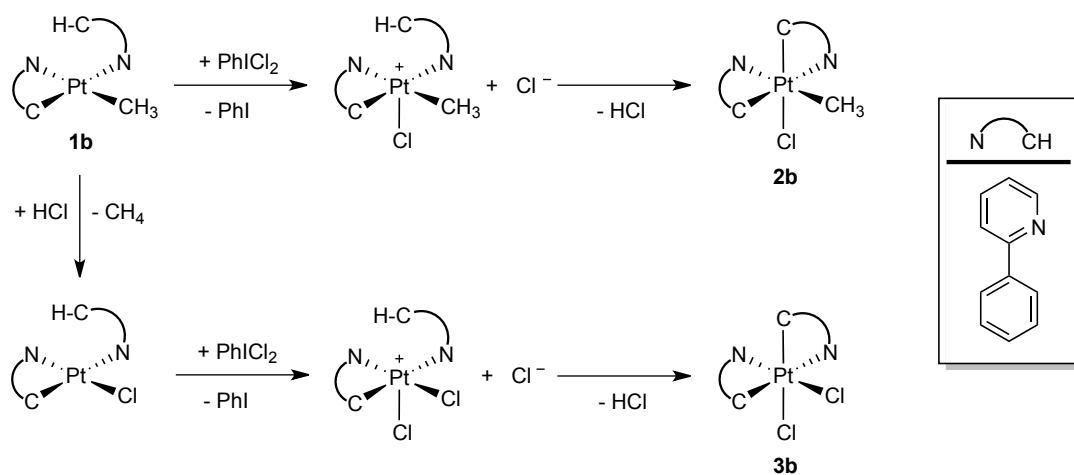
1.7. Effect of HCl in the reaction of **1b** with PhICl₂

The intermediate **1b** was isolated in order to study its reactivity toward PhICl₂ and optimize the conditions for the synthesis of complexes **2**. When the reaction of **1b** with PhICl₂ was carried out in the absence of a base (Scheme S1, **a**), a mixture of **2b** and [Pt(ppy)₂Cl₂] (**3b**) is obtained. Complex **3b** has been previously reported⁸ and was identified by its ¹H-NMR data. In the presence of an external base (DIPEA), only **2b** is formed (Scheme S1, **b**), while in the presence of HCl, generated *in situ* from trimethylsilyl chloride (TMSCl) and water, complex **3b** is obtained as the major product (Scheme S1, **c**).



Scheme S1. Effect of HCl in the reaction of **1b** with PhICl₂. DIPEA = *N,N*-diisopropylethylamine; TMSCl = trimethylsilyl chloride.

Plausible reaction paths for the formation of **2b** and **3b** are outlined in Scheme S2. The metalation of the pendant phenyl moiety in **1b** produces HCl, which can then react with other molecules of **1b** to give a Pt(II) chlorocomplex and methane. The reaction of methylplatinum(II) complexes with strong acids HX at room temperature is known to involve the oxidative addition of HX to give a Pt(IV) compound that subsequently undergoes the reductive elimination of methane, resulting in the substitution of the methyl ligand for X. The subsequent reaction of the Pt(II) chlorocomplex with PhICl₂ then leads to **3b**.⁹



Scheme S2. Proposed reaction paths for the formation of **2b** and **3b** from the reaction of **1b** with PhICl_2 .

2. Photophysical data

2.1. Electronic absorption data of 2a-i

Table S6. Absorption data of **2a-i** in CH₂Cl₂ (*ca.* 5 × 10⁻⁵ M) at 298 K.

Complex	$\lambda_{\text{max}}/\text{nm}$ ($\epsilon \times 10^{-3} / \text{M}^{-1}\text{cm}^{-1}$)
2a	255 (23.4), 303 (16.3), 322 (12.7, sh)
2b	263 (25.0), 306 (14.9), 320 (12.7), 332 (11.8, sh)
2c	268 (22.6), 312 (14.2), 326 (14.7), 336 (13.4, sh)
2d	280 (22.1), 334 (24.5)
2e	290 (17.1), 322 (27.1, sh), 358 (40.6), 371 (36.9, sh)
2f	295 (32.0), 303 (34.2), 327 (28.2), 352 (47.3), 366 (51.5)
2g	289 (24.3), 346 (18.6), 355 (17.1, sh)
2h	340 (14.2, sh), 362 (18.3), 376 (16.2)
2i	260 (48.4, sh), 308 (11.0), 337 (15.6), 363 (17.6), 378 (16.9)

2.2. Excitation and emission spectra of 2a-i at 298 K

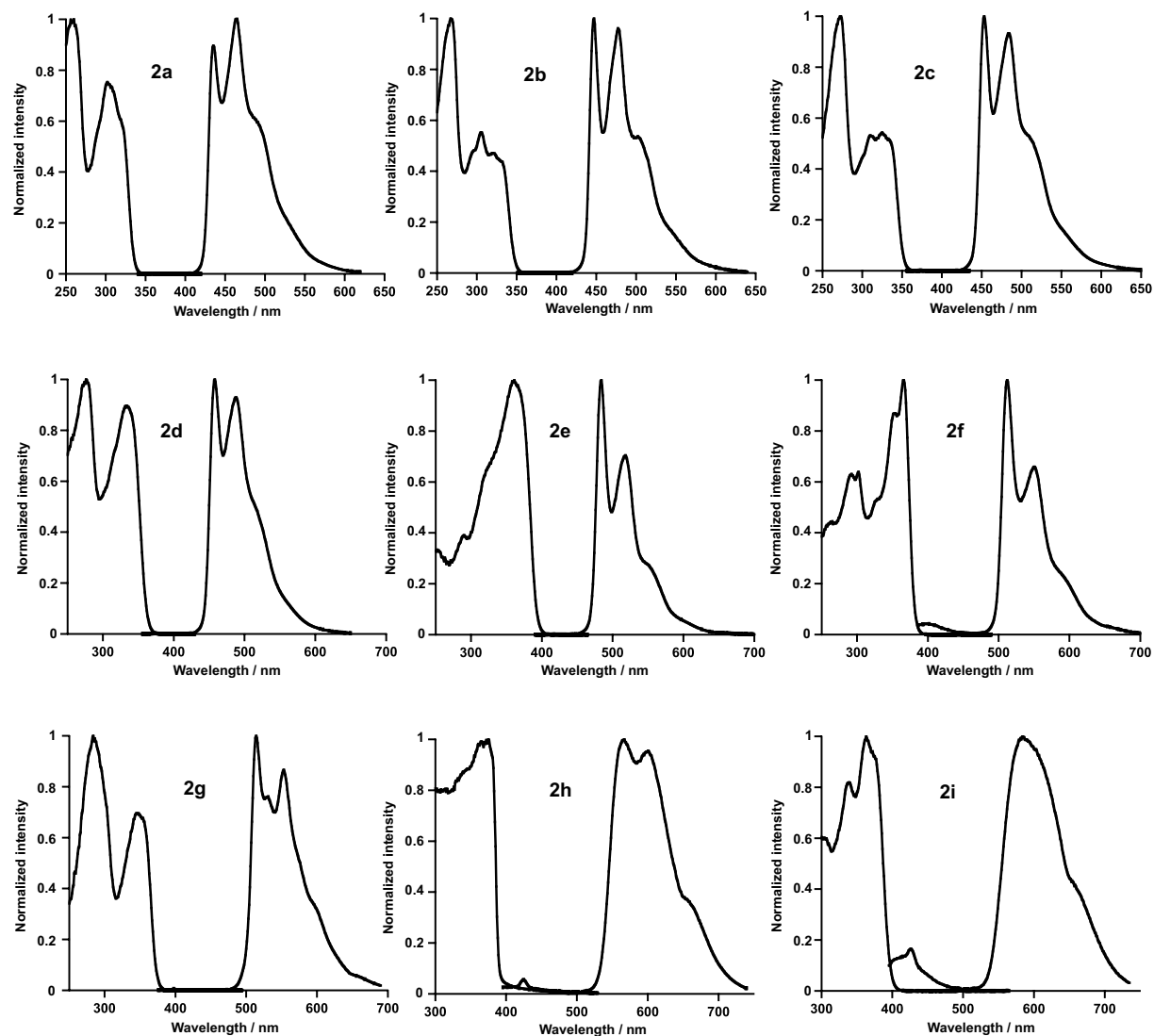


Figure S5. Excitation and emission spectra of **2a-i** in CH_2Cl_2 at 298 K.

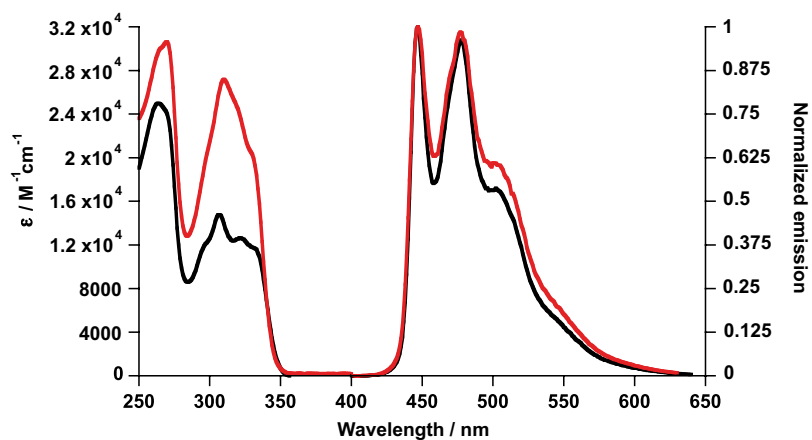


Figure S6. Comparison of absorption and emission spectra of **2b** (black line) and *fac*-[Pt(ppp)₃]OTf (red line) in CH_2Cl_2 at 298 K.

2.3. Emission spectra of 2a-i at 77 K

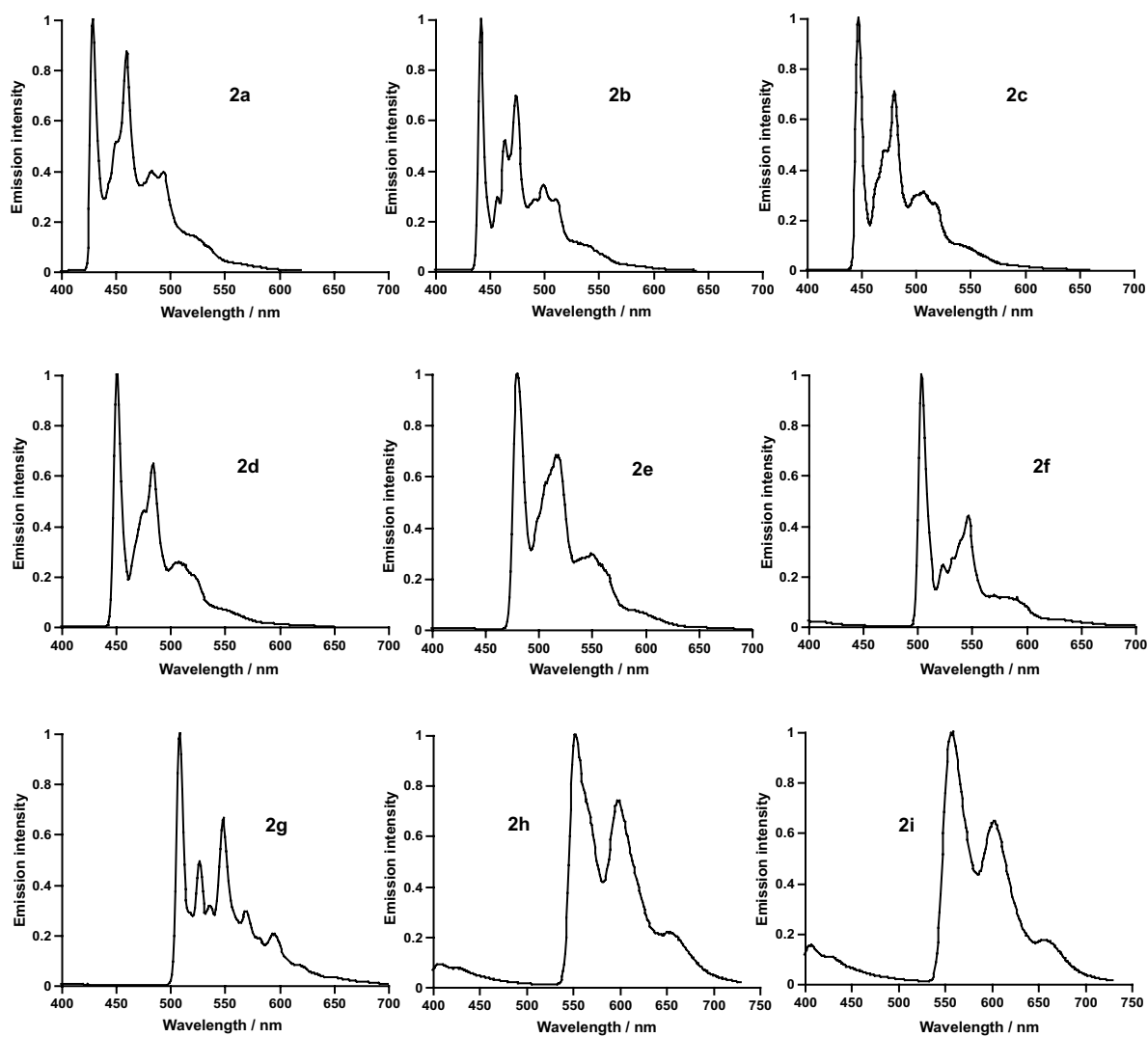


Figure S7. Emission spectra of **2a-i** in PrCN frozen glasses at 77 K.

2.4. Effect of the concentration on the emission of **2b** in solution

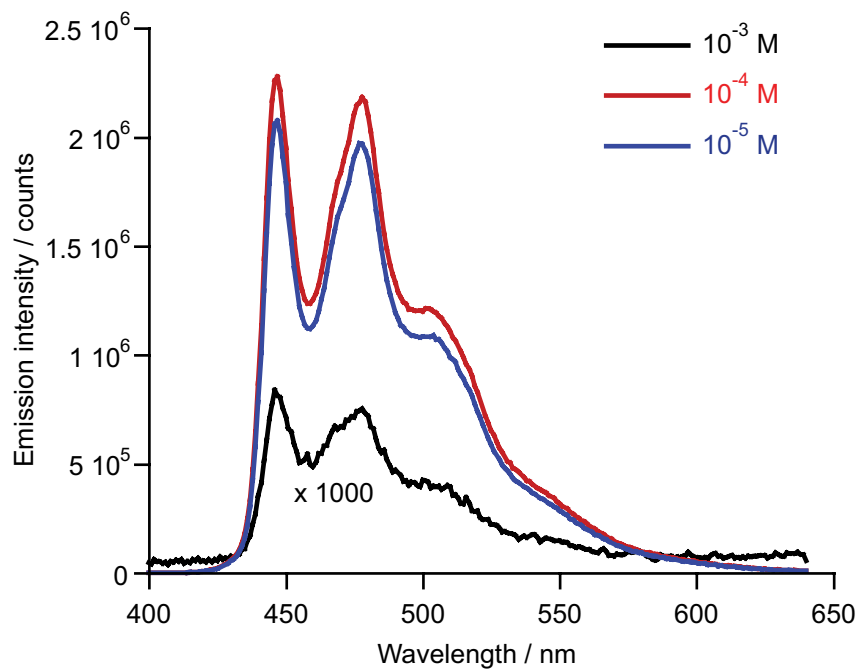


Figure S8. Emission spectra of **2b** in CH_2Cl_2 solution at different concentrations at 298 K.

3. Electrochemical characterization of **2b**

The cyclic voltammogram of **2b** was registered with a potentiostat/galvanostat AUTOLAB-100 (Echo-Chemie, Utrecht), employing a three-electrode electrochemical cell equipped with a glassy carbon working electrode (Metrohm, 2 mm diameter), an Ag/AgCl/3 M KCl electrode reference, and a glassy carbon rod counter electrode. The measurements were carried out at 298 K under an argon atmosphere, using degassed 1 mM solutions of the complex in extra-dry MeCN (Acros Organics) and 0.1 M (Bu₄N)PF₆ as the electrolyte. Prior to each measurement, the working electrode was polished with alumina slurry (0.05 μm) and rinsed with water and acetone. The electrodes were activated electrochemically in the background solution by means of several voltammetric cycles at 1 V s⁻¹ between -2.7 V and 2.2 V. At the end of the measurement, the reference electrode was checked against the ferricinium/ferrocene (Fc⁺/Fc) redox couple [0.40 V vs. the standard calomel electrode (SCE) in MeCN]. HOMO/LUMO energies were estimated from the onset values of the oxidation and reduction waves referenced against the Fc⁺/Fc couple, using a formal potential of 5.1 eV for this couple in the Fermi scale:¹⁰

$$E_{\text{HOMO}} = -(E_{\text{onset, ox}} + 5.1 - 0.4) \text{ eV}; E_{\text{LUMO}} = -(E_{\text{onset, red}} + 5.1 - 0.4) \text{ eV}$$

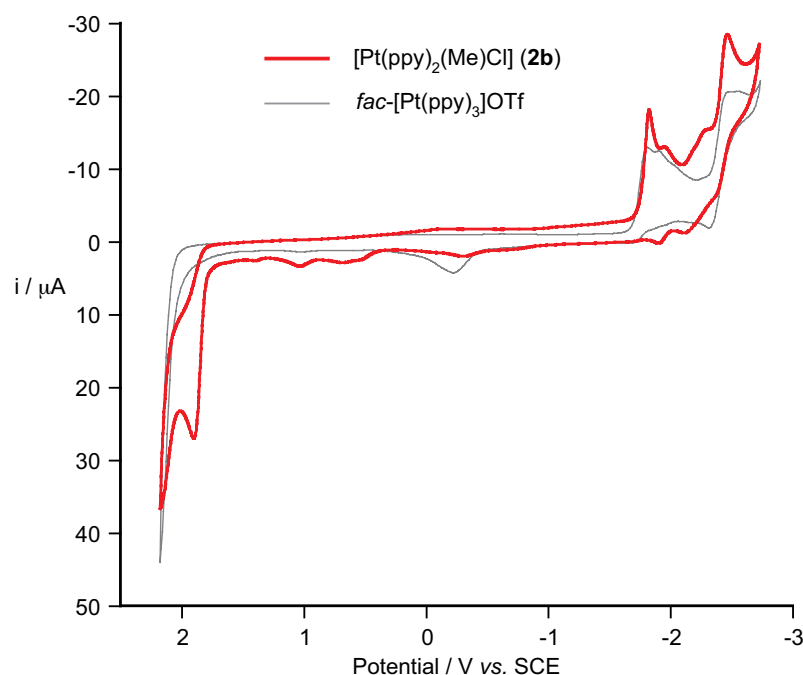


Figure S9. Cyclic voltammogram of complex **2b** in MeCN at 100 mV s⁻¹. The voltammogram of *fac*-[Pt(ppy)₃]OTf¹¹ under the same conditions is included for comparison.

4. Photostability experiments

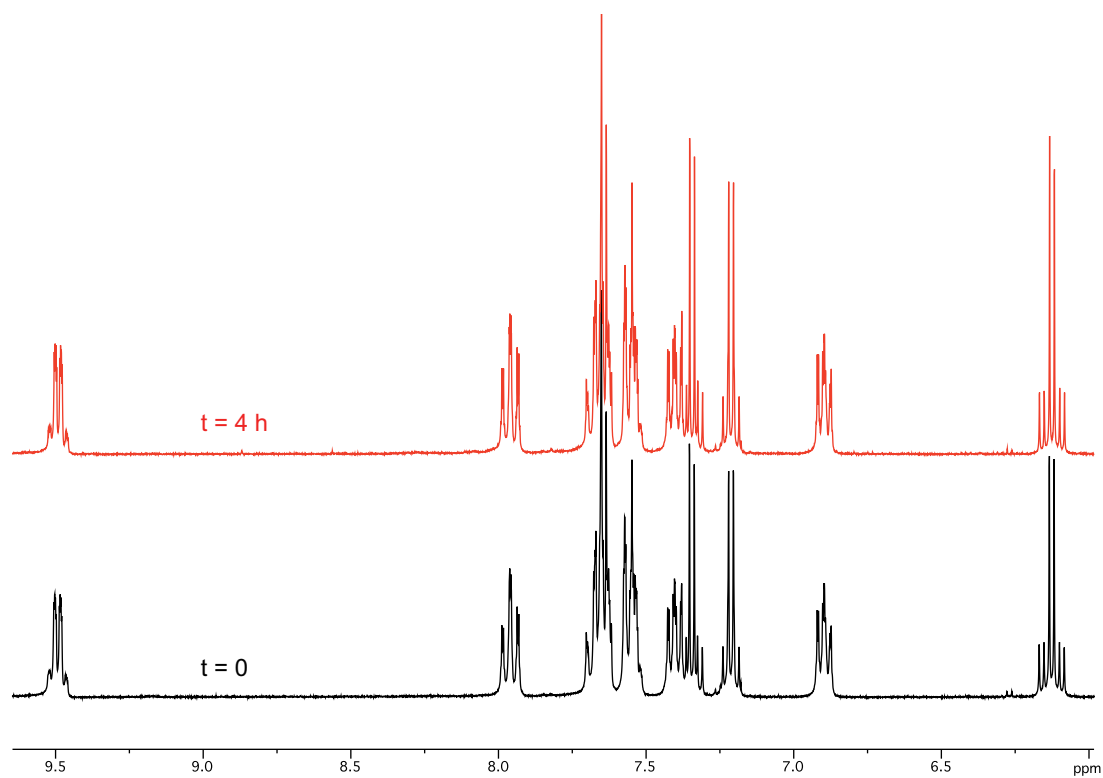


Figure S10. ¹H-NMR spectra of **2g** in CD₂Cl₂ before and after irradiation with a 36 W Philips UVB Narrowband Lamp (310 nm).

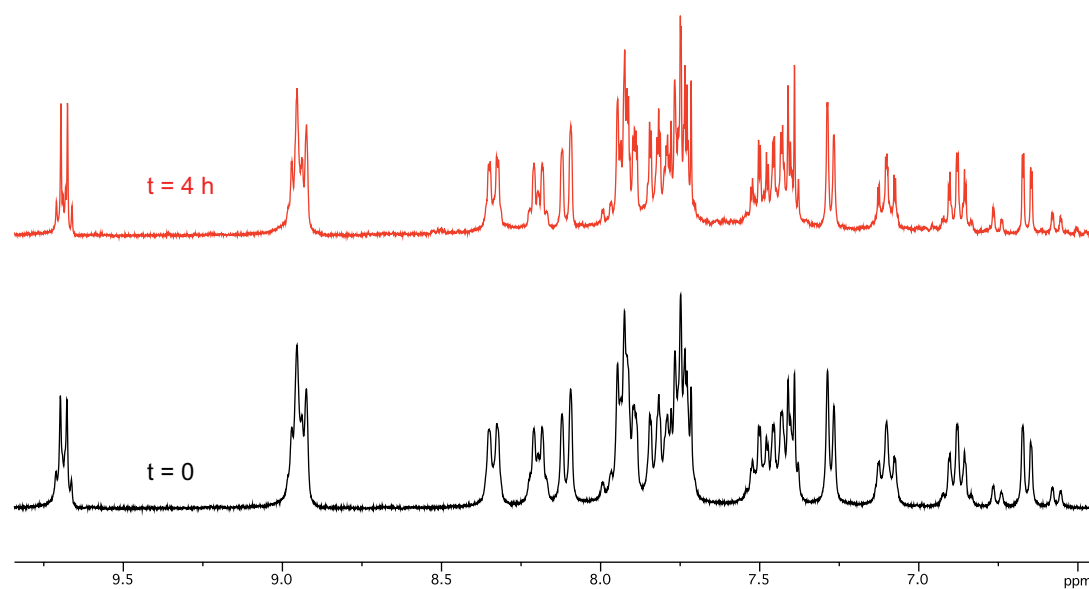


Figure S11. ¹H-NMR spectra of **2h** in CD₂Cl₂ before and after irradiation with a 36W Philips UVB Narrowband Lamp (310 nm).

5. References

- 1 G. S. Hill, M. J. Irwin, C. J. Levy, L. M. Rendina, R. J. Puddephatt, R. A. Andersen and L. McLean, in *Inorganic Syntheses*, ed. M. Y. Darensbourg, John Wiley & Sons, Inc., 1998, pp. 149.
- 2 D. C. Powers, D. Benitez, E. Tkatchouk, W. A. Goddard and T. Ritter, *J. Am. Chem. Soc.*, 2010, **132**, 14092.
- 3 H. Mizuno, J. Takaya and N. Iwasawa, *J. Am. Chem. Soc.*, 2011, **133**, 1251.
- 4 X. Yang, N. Sun, J. Dang, Z. Huang, C. Yao, X. Xu, C.-L. Ho, G. Zhou, D. Ma, X. Zhao and W.-Y. Wong, *J. Mater. Chem. C*, 2013, **1**, 3317.
- 5 A. Tsuboyama, H. Iwawaki, M. Furugori, T. Mukaide, J. Kamatani, S. Igawa, T. Moriyama, S. Miura, T. Takiguchi, S. Okada, M. Hoshino and K. Ueno, *J. Am. Chem. Soc.*, 2003, **125**, 12971.
- 6 N. Tian, A. Thiessen, R. Schiewek, O. J. Schmitz, D. Hertel, K. Meerholz and E. Holder, *J. Org. Chem.*, 2009, **74**, 2718.
- 7 G. M. Sheldrick, *Acta Crystallogr., Sect. A: Found. Crystallogr.*, 2008, **64**, 112.
- 8 S. R. Whitfield and M. S. Sanford, *Organometallics*, 2008, **27**, 1683.
- 9 (a) G. S. Hill, L. M. Rendina and R. J. Puddephatt, *Organometallics*, 1995, **14**, 4966; (b) S. S. Stahl, J. A. Labinger and J. E. Bercaw, *J. Am. Chem. Soc.*, 1996, **118**, 5961; (c) F. Zhang, E. M. Prokopchuk, M. E. Broczkowski, M. C. Jennings and R. J. Puddephatt, *Organometallics*, 2006, **25**, 1583; (d) Z. M. Hudson, B. A. Blight and S. Wang, *Org. Lett.*, 2012, **14**, 1700.
- 10 C. M. Cardona, W. Li, A. E. Kaifer, D. Stockdale and G. C. Bazan, *Adv. Mater.*, 2011, **23**, 2367.
- 11 F. Juliá, G. Aullón, D. Bautista and P. González-Herrero, *Chem. Eur. J.*, 2014, **20**, 17346.